Capturing first- and second-order behavior in magnetocaloric $CoMnSi_{0.92}Ge_{0.08}$

K. Morrison,[1] J. D. Moore,[1] K. G. Sandeman,[2] A. D. Caplin,[1] and L. F. Cohen[1]
[1]*The Blackett Laboratory, Imperial College, London SW7 2AZ, United Kingdom*
[2]*Department of Material Science and Metallurgy, University of Cambridge, Cambridge CB2 3QZ, United Kingdom*
(Received 15 January 2009; revised manuscript received 6 March 2009; published 6 April 2009)

Here we examine the constituent components that make a magnetocaloric material attractive for application. The field-temperature phase diagram is studied and using calorimetry, the first-order and second-order components of the magnetic field-driven magneto-structural phase transition in $CoMnSi_{0.92}Ge_{0.08}$ are extracted. It is demonstrated that below 262 K the transition shows a latent heat component associated with first-order behavior when the material changes from antiferromagnetic to ferromagnetic order. Such a transition is known as a metamagnetic transition. We identify 262 K as a tricritical point and above this temperature T_{crit} the transition shows only continuous, second-order characteristics. Hall-probe imaging that has a five micron pixel resolution is then used to study the striking differences in the spatial evolution of the transition above and below T_{crit}. We demonstrate that the hysteresis of the transition is linearly related to the magnitude of the latent heat; an observation that has important implications for the use of this and other first-order systems for application as magnetic refrigerants.

DOI: 10.1103/PhysRevB.79.134408 PACS number(s): 75.30.Sg, 75.30.Kz

I. INTRODUCTION

Whether a phase transition is first order or continuous is crucial to many phenomena found in nature. Recently, a new class of magnetocaloric materials which undergo a field-driven magneto-structural phase transition from one form of magnetic order to another with an associated "giant" change of entropy have been reported.[1–5] With the discovery of these giant magnetocaloric effects (GMCE) (Refs. 3, 6, and 7), the possible application of the MCE for environmentally friendly and energy efficient room-temperature refrigeration has been brought much closer. Consequently, research into room-temperature magnetocaloric materials has grown dramatically over the last decade[1,8] and is of increasing and pressing importance.

The majority of the current most promising contenders as refrigerant materials exhibits magnetostructural coupling, that is, coincident magnetic and structural phase transitions,[9,10] leading to an increase in the magnetocaloric effect due to the first-order nature of such transitions. However, this leads to hysteresis, which is unattractive for applications because it introduces energy dissipation. It appears that the hysteresis of the field-driven magnetic transition can be reduced when materials are made using particular processing routes suggesting that morphology and defects may play a strong role.[3,11–13] These observations are encouraging because one of the major questions is whether it is possible to engineer a material so that the physical properties attractive for application can be maximized (large entropy change due to a first-order transition), while those that are detrimental (hysteresis) can be suppressed. In this paper we examine the role of hysteresis and its relationship to the strength of the first-order transition in the inverse[14] magnetocaloric material $CoMnSi_{0.92}Ge_{0.08}$.

II. EXPERIMENTAL DETAILS

Ingots were prepared by induction melting stoichiometric amounts of elemental powders and annealing for 60 h at 950 °C followed by slow cooling. The annealing and slow-cooling process was carried out to retain single phase structure.[15] X-ray diffraction and Rietveld refinement using an internal Si standard yielded a good fit to a single phase, orthorhombic *Pnma* structure with lattice parameters of $a=5.8716$ Å, $b=3.6980$ Å, and $c=6.8709$ Å.[15] Samples that were imaged were prepared by polishing using varying grades of diamond paste.

All magnetization and Hall imaging[16] measurements were carried out in an Oxford instrument Vibrating Sample Magnetometer, capable of reaching fields of ± 4 T and temperatures ranging from 4.2–295 K. For local *M-H* loops, the change in Hall voltage measured at a single point was tracked as a function of field. To obtain comparable data the local loops were normalized to the saturation moment of the bulk sample at the same temperature.

Latent heat[17] and heat capacity[18] measurements were carried out on approximately 100-μm^3-sized fragments (typically $100\times 50\times 100$ μm^3), using a SiNi membrane sensor in an 8 T magnet. The isothermal entropy changes from magnetization ΔS_M,[19] heat-capacity ΔS_C, and latent heat ΔS_{LH}, were derived using Eqs. (1)–(3), where $C_{H1,2}$ is the heat capacity at fields H_1 and H_2 taken here as 0 and 8 T, respectively, ΔQ is the heat absorbed by the sample at a given temperature, and T1 is a reference temperature used for integration. Further details of this method and subsequent calculations can be found elsewhere.[17,20]

$$\Delta S_M = \int_{H1}^{H2} \frac{\partial M}{\partial T} dH, \tag{1}$$

$$\Delta S_C = \int_{T1}^{T} \frac{C_{H2} - C_{H1}}{T} dT, \tag{2}$$

$$\Delta S_{LH} = \frac{\Delta Q}{T}. \tag{3}$$

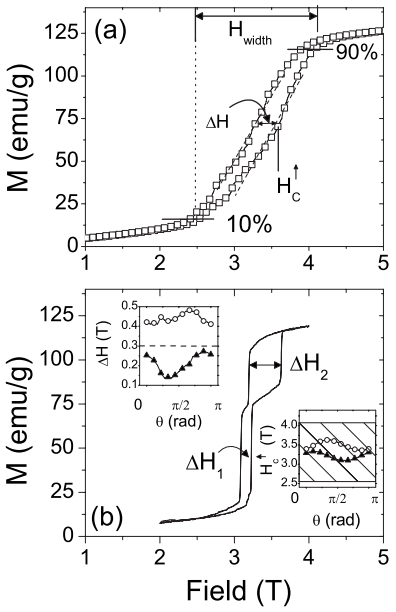

FIG. 1. Magnetic behavior of bulk and micrometer sized fragments of $CoMnSi_{0.92}Ge_{0.08}$ at 230 K. (a) *M-H* loop of a ~1 mm^3 bulk sample—see the text for definitions and (b) *M-H* loop of a ~200-μm^3-sized fragment suggesting the presence of two crystallites with individual critical fields $H_c^{\uparrow,\downarrow}$. Lower inset: Angular variation of $H_c^{\uparrow}(\theta)$, defined as the mid-point of the transition of each crystallite, 1 (▲) and 2 (○), identified in the fragment, as a function of angle with respect to the applied field. The shaded region indicates H_{width} of the bulk material. Upper inset: Angular variation of the hysteresis width associated with the crystallite, ΔH_1 (▲) and ΔH_2 (○), as a function of angle; the dotted line indicates the hysteresis width observed in the bulk, which is, as expected, independent of field angle.

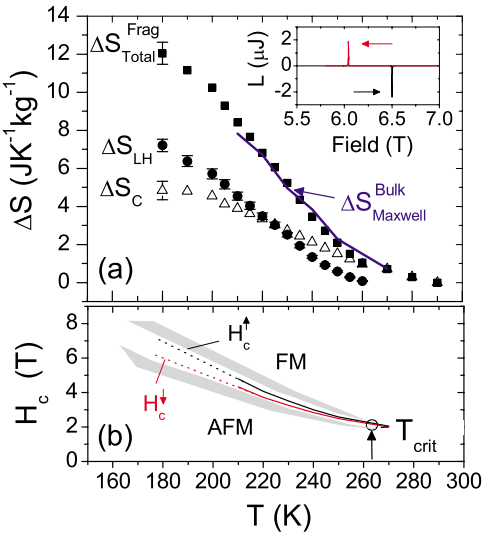

FIG. 2. (Color online) Temperature dependence of the entropy change. (a) Total entropy change (for a field change of 0–8 T) calculated from calorimetry, ΔS_{Total} (-■-), of a 100 μm fragment, compared to results from bulk magnetization measurements, $\Delta S_{\text{Maxwell}}$ (-). ΔS_{Total} consists of latent heat, ΔS_{LH} (-●-), and heat capacity, ΔS_C (-△-), contributions. Error bars at 180 K are indicative of the errors at all temperatures. Inset shows latent heat data taken from the fragment at 180 K where there is a single spike associated with the transition in each field direction. (b) H_c-T schematic constructed from bulk magnetometry (-) and latent heat (- - -) measurements, where the lower line corresponds to $H_c^{\downarrow}$ and the upper line $H_c^{\uparrow}$. We identify the tricritical point, T_{crit}, as the temperature at which ΔH and the latent heat reach zero, below which phase coexistence occurs (gray shaded area).

III. RESULTS AND DISCUSSION

Previous work has shown how the Curie transition T_c between ferromagnetic and paramagnetic states, as well as the field-driven metamagnetic phase transition from low-field antiferromagnetic (AFM) order to high-field ferromagnetic (FM) order, evolves with Ge doping in the $CoMnSi_{1-x}Ge_x$ system (the latter transition is referred to in that paper as T_t).[15] For x=0.08 studied here, $T_c \sim 420$ K and $T_t \sim 375$ K in zero external magnetic field and as magnetic field is applied these temperatures diverge away from one another (T_c increases in field and T_t is lowered in field) due to the stabilization of the FM state.

Figure 1 summarizes the magnetization-field (*M-H*) loop at 230 K of a "bulk" (~1 mm^3) polycrystalline sample and a ~200 μm^3 fragment of $CoMnSi_{0.92}Ge_{0.08}$. We define the critical field, H_c, as the point at which the magnetization, M, is 50% of its saturation value, and write $H_c^{\uparrow}$ for increasing and $H_c^{\downarrow}$ for decreasing magnetic-field directions, respectively. The difference in field between $H_c^{\uparrow}$ and $H_c^{\downarrow}$ is the hysteresis width, ΔH. The transition width, $H_{\text{width}}^{\uparrow}$ and $H_{\text{width}}^{\downarrow}$, is defined here as the field required to go from 10% to 90% of the saturation moment of the sample as the field is increased or decreased.[21] A schematic H_c-T phase diagram is shown in Fig. 2 and is constructed in part from the global magnetization data as well as from latent heat data as discussed below.

Note that the 230 K *M-H* loop shown in Fig. 1(a) for the bulk sample displays a broad and smooth transition, normally associated with second-order behavior, but with finite hysteresis ΔH (i.e., $H_c^{\uparrow} \neq H_c^{\downarrow}$) usually indicative of a first-order phase transition. When small fragments of the order of 100 microns are taken from the bulk and studied individually, the magnetic behavior is quite different. Figure 1(b) shows that the *M-H* loop of a typical fragment exhibits two sharp, steplike transitions, suggesting the presence of two crystallites which undergo first-order transitions, oriented differently with respect to each other, therefore with different critical fields. The lower inset in Fig. 1(b) shows the critical field, $H_c^{\uparrow}(\theta)$, of these individual "crystallites" in the fragment plotted as a function of angle, θ, between the applied field and the broad-fragment surface. The shaded region encompassing the $H_c^{\uparrow}(\theta)$ of the two crystallites indicates the transition width, H_{width}, of the bulk sample. Analogous to single domain ferromagnets, these fragments are apparently small enough that they switch sharply from one phase to the other. The bulk *M-H* loop appears broad because in this system the magnetocrystalline anisotropy produces a distribution of $H_c^{\uparrow,\downarrow}$ in the randomly-oriented fragments that make up the bulk material. The broad H_{width} of the bulk material compared to the angular variation in $H_c^{\uparrow,\downarrow}$ suggests that other factors, such as strain or local inhomogeneity may also influence the transition. Interestingly the hysteresis width, ΔH, of the indi-

vidual crystallite varies as a function of field angle [Fig. 1 (upper inset)], unlike the angle independence of the bulk ΔH (flat dotted line). These results highlight the role of magnetocrystalline anisotropy on the key parameters $H_c^{\uparrow,\downarrow}$ and ΔH in this system.

The isothermal entropy changes derived from calorimetric measurements of an approximately 100 μm^3 fragment and from magnetometry of the bulk sample, for a field change of 0–8 T, are shown in Fig. 2. Note that the total entropy change determined from the bulk and fragment data agree well. As the temperature is increased, the entropy change due to the latent heat contribution, ΔS_{LH} decreases until it reaches zero at 262 K, so that the magnetocaloric effect above 262 K arises only from a second-order transition. The combined calorimetric and bulk magnetometry data allow us to construct the schematic H_c-T phase diagram shown in Fig. 2(b) which we referred to previously. At temperatures below the tricritical point, T_{crit}, there is a first-order AFM to FM transition, indicated by a significant $\Delta S_{LH.}$, accompanied by hysteresis. Phase coexistence occurs where there is a latent heat associated with a nucleation energy barrier, inherent to first-order phase transitions; the latent heat disappears at T_{crit} =262 K. Above T_{crit} the second-order AFM-FM phase-transition results in a small entropy change (<1 JK^{-1} kg^{-1}) until T_t(=375 K) is reached.

Hall-probe imaging of the magnetic field-driven phase transition can provide additional insight because of the opportunity to investigate magnetic behavior at individual sites (governed by pixel resolution, i.e., the size of the Hall probe used). We call the M-H loops constructed from individual sites "local loops." A selection of images of a 1 mm^2 surface area at 230 K and 296 K are given in Figs. 3(a) and 3(b), respectively. Figure 3 also shows the M-H loop of the bulk sample and of an individual pixel, i.e., a local loop. The difference in the transition behavior at the two chosen temperatures is striking: At 230 K the phase transition is first order and hysteretic. Note that although the M-H loop shows a gradual transition in the bulk sample, on a spatially local scale both H_{width} and ΔH are much smaller, similar to the contrast between bulk and fragment samples in Fig. 1. The switching of magnetic moment over well defined spatial regions can be described by a nucleation process. The magnetic images demonstrate that there is a distribution of $H_c^{\uparrow,\downarrow}$ across the sample, and different sites nucleate the new magnetic phase at different fields. This is the manifestation of phase coexistence across the transition in direct correspondence with the large H_{width} observed in the bulk sample at this temperature (Fig. 1).

At 296 K the field-driven transition is second order. The images taken in increasing and decreasing field are now identical, reflecting that ΔH=0 both globally and locally. Unlike the switching behavior at 230 K, the local M-H loops at every pixel site on the sample are coincident with the bulk M-H loop, indicating that the local behavior is everywhere identical to the global magnetization. This is indeed the usual manifestation of a second-order transition; the change from one magnetic order to another is smooth, gradual, and spatially uniform.

We now turn to examine the important relationship between hysteresis and entropy change. Figure 4 shows that

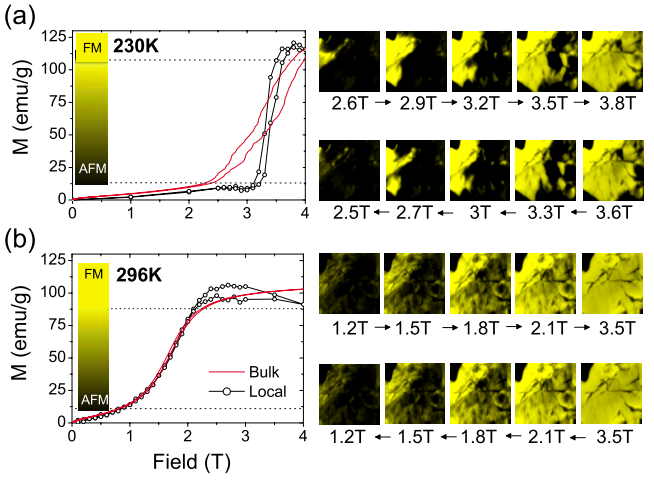

FIG. 3. (Color online) Hall-probe imaging of $CoMnSi_{0.92}Ge_{0.08}$ across the field-driven magnetic transition: (a) first-order transition at 230 K, (b) second-order transition at 296 K. Left: The M-H loops constructed from a single pixel (-○-) of a series of images are shown at these temperatures alongside bulk measurements (−). Right: Equivalent up-field and down-field images are shown to highlight reversibility of this sample. Each image is 1 mm across. The color scale is set to black at 10% of saturation (AFM state), and white (yellow online) at 90% saturation (FM state). Dark areas in the magnetically saturated images indicate the presence of cracks in the sample surface or the sample edge (top left corner), which were used as location markers.

there is a linear relationship between the magnetic hysteresis, ΔH, and the latent heat, ΔQ, of a single latent heat spike. Due to the development of multiple spikes as the temperature

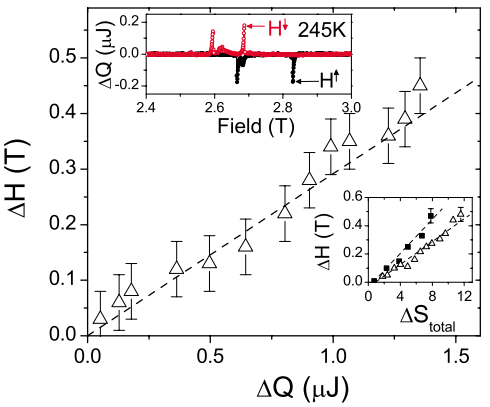

FIG. 4. (Color online) Relationship between hysteresis and entropy change. Main figure: Hysteresis associated with a single latent heat spike (identified in upper inset by the arrows; ΔH=$H^{\uparrow}$-$H^{\downarrow}$) plotted as a function of latent heat, ΔQ. Upper inset: Example of how the transition "breaks up" into multiple latent heat spikes at high temperatures. Note that ΔS_{LH} is determined as the sum of these spikes. Lower inset: Hysteresis, ΔH, of bulk (■) and fragment (△) plotted as a function of total entropy change calculated using the Maxwell relation (see methods section for details). The lines are guides for the eye and the error scale has been indicated on one of the points. In this case we have estimated ΔH using the average over multiple latent heat spikes that appear as the temperature is increased.

was increased, (as demonstrated by the upper inset of Fig. 4), this was determined for a single latent heat spike, tracked as a function of temperature. To compare this to the data available for the bulk sample, the hysteresis width, ΔH, has also been compared to the total entropy change, ΔS_{total} $(=\Delta S_{\text{LH}} + \Delta S_C)$ because for the bulk sample we can only use the magnetization data to calculate ΔS_{total}. We find that ΔH is proportional to ΔS_{total} (lower inset, Fig. 4), as indicated by the lines drawn but the slope, denoted here as γ, is different for the bulk ($\gamma \approx 0.65$ TK kg J^{-1}) and for the fragment ($\gamma \approx 0.46$ TK kg J^{-1}). The x-intercept of the slopes occurs around 1 JK^{-1} kg^{-1}, as expected from Fig. 2, where the remaining entropy change at T_{crit} was shown to be approximately 1 JK^{-1} kg^{-1}.

The question remaining relates to understanding the different γ values found for bulk and fragment. As ΔS_{total} agreed well for bulk and fragment (Fig. 2) we can assume that the difference in γ is not due to varying contributions of ΔS_{LH} to ΔS_{total}. There is, however, a difference in $H_c^{\uparrow,\downarrow}$ of the bulk and fragment at 230 K consistent with the variation shown in Fig. 1 of 0.1 T between the mean and easy axis alignment. Hence we draw the conjecture that the different γ values indicate the role that magnetic anisotropy might play in these materials: for the same entropy change a smaller hysteresis was observed in the fragment, most likely as a result of its orientation. This suggests that manipulating magnetic anisotropy could hold one of the keys to changing these materials favorably.

The observation that the hysteresis varies linearly with the magnitude of the latent heat has some important implications which we can draw attention to by considering how the Gibbs free-energy profile, F(M), changes as the latent heat decreases for a metastable system with two energy minima.[22] The horizontal separation of the minima (ΔM) defines the magnitude of the latent heat jump (change of order parameter), and the barrier (ΔE) defines the lower bound for the hysteresis. Our observation is that in the system we have studied here as the latent heat increases so does the energy barrier, and that these are correlated. In order to manipulate ΔH, there has to be some compromise (depression) of the first-order nature of the transition, or manipulation of the factor γ, which as we have shown can be closely dependent on the magnetic anisotropy.

IV. CONCLUSION

We have shown that the metamagnetic transition in first-order magneto-structural materials is complex and needs to be studied on different lengthscales in order to be better understood. The sharp changes in magnetization at high spatial scale are indeed a direct manifestation of the first-order magnetic transition, which is driven in large samples by a nucleation process. The broad and continuous *M-H* loops observed from global magnetometry at 230 K average many such sharp loops. We have also shown that magnetic anisotropy plays a role and in a polycrystalline bulk sample the random orientation of crystallites in the bulk are predominantly responsible for the distribution of $H_c^{\uparrow,\downarrow}$ and ΔH. The room-temperature Hall probe images show how a smooth and continuous field-driven phase transition is manifest in striking contrast to the first-order behavior at 230 K. We correlate hysteresis with the magnitude of the latent heat jump, and our observations suggest that manipulating the magnetocrystalline anisotropy might be one route to controlling hysteresis without significant impairment of the magnitude of the magnetocaloric effect. These observations form a basis for a fundamental understanding of these field-driven transitions at a local spatial scale and provide insight for materials engineering that could lead to significantly improved magnetocaloric systems for applications.

ACKNOWLEDGMENTS

This work was supported by EPSRC-GB Platform under Grant No. EP/E016243/1—A Platform to Develop and Utilize Characterization Tools for Functional Magnetic Materials. K.G.S. would like to acknowledge S. Özcan and K. Roberts for help with sample preparation, G. G. Lonzarich for the use of sample synthesis facilities, and The Royal Society and the EPSRC-GB under Grant No. GR/R72235/01 for financial support.

[1] K. A. Gschneidner, Jr., V. K. Pecharsky, and A. O. Tsokol, Rep. Prog. Phys. **68**, 1479 (2005).
[2] V. K. Pecharsky and K. A. Gschneidner, Jr., Phys. Rev. Lett. **78**, 4494 (1997).
[3] A. de Campos, D. L. Rocco, A. M. G. Carvalho, L. Caron, A. A. Coelho, S. Gama, L. M. da Silva, F. C. G. Gandra, A. O. dos Santos, L. P. Cardoso, P. J. von Ranke, and N. A. de Oliveira, Nature Mater. **5**, 802 (2006).
[4] P. J. von Ranke, N. A. de Oliveira, C. Mello, A. M. Carvalho, and S. Gama, Phys. Rev. B **71**, 054410 (2005).
[5] G. J. Liu, J. R. Sun, J. Lin, Y. W. Xie, T. Y. Zhao, H. W. Zhang, and B. G. Shen, Appl. Phys. Lett. **88**, 212505 (2006).
[6] S. Gama, A. A. Coelho, A. de Campos, A. M. Carvalho, F. C. G. Gandra, P. J. von Ranke, and N. A. de Oliveira, Phys. Rev. Lett. **93**, 237202 (2004).
[7] V. K. Pecharsky and K. A. Gschneidner, Jr., Adv. Mater. **13**, 683 (2001).
[8] V. K. Pecharsky and K. A. Gschneidner, J. Magn. Magn. Mater. **200**, 44 (1999).
[9] V. K. Pecharsky, A. P. Holm, K. A. Gschneidner, Jr., and R. Rink, Phys. Rev. Lett. **91**, 197204 (2003).
[10] V. K. Pecharsky, K. A. Gschneidner, Jr., Y. Mudryk, and D. Paudyal, J. Magn. Magn. Mater. (to be published).
[11] O. Gutfleisch, A. Yan & K. H. Müller, J. Appl. Phys. **97**, 10M305 (2005).
[12] V. Provenzano, A. J. Shapiro, and R. D. Shull, Nature (London) **429**, 853 (2004).
[13] T. Zhang, Y. Chen, and Y. Tang, J. Phys. D **40**, 5778 (2007).

[14] T. Krenke, E. Duman, M. Acet, E. F. Wassermann, X. Moya, L. Manosa, and A. Planes, Nature Mater. **4**, 450 (2005).
[15] K. G. Sandeman, R. Daou, S. Özcan, J. H. Durrell, N. D. Mathur, and D. J. Fray, Phys. Rev. B **74**, 224436 (2006).
[16] J. D. Moore, G. K. Perkins, Y. Bugoslavsky, L. F. Cohen, M. K. Chattopadhyay, S. B. Roy, P. Chaddah, K. A. Gschneidner, and V. K. Pecharsky, Phys. Rev. B **73**, 144426 (2006).
[17] Y. Miyoshi, K. Morrison, J. D. Moore, D. A. Caplin, and L. F. Cohen, Rev. Sci. Instrum. **79**, 074901 (2008).
[18] A. A. Minakov, S. B. Roy, Y. V. Bugoslavsky, and L. F. Cohen, Rev. Sci. Instrum. **76**, 043906 (2005).
[19] V. K. Pecharsky, K. A. Gschneidner, Jr., A. O. Pecharsky, and A. M. Tishin, Phys. Rev. B **64**, 144406 (2001).
[20] K. Morrison, Y. Miyoshi, J. D. Moore, A. Barcza, K. G. Sandeman, A. D. Caplin, and L. F. Cohen, Phys. Rev. B **78**, 134418 (2008).
[21] J. D. Moore, G. K. Perkins, Y. Bugoslavsky, M. K. Chattopadhyay, S. B. Roy, P. Chaddah, V. K. Pecharsky, K. A. Gschneidner, Jr., and L. F. Cohen, Appl. Phys. Lett. **88**, 072501 (2006).
[22] M. D. Kuz'min and M. Richter, Phys. Rev. B **76**, 092401 (2007).